TELKOMNIKA, Vol.12, No.2, June 2014, pp. 419~428
ISSN: 1693-6930, accredited A by DIKTI, Decree No: 58/DIKTI/Kep/2013
DOI: 10.12928/TELKOMNIKA.v12i2.2089

Planar Finger-Shaped Antenna Used in Ultra-Wideband Wireless Systems

Rashid A. Fayadh[1], Mohd Fareq A. Malek[2], Hilal A. Fadhil[1], Fwen Hoon Wee[1]
[1] School of Computer and Communication Engineering, Universiti Malaysia Perlis (UniMAP), 02000 Arau, Perlis, Malaysia
[2] School of Electrical Systems Engineering, Universiti Malaysia Perlis (UniMAP), 02600 Arau, Perlis, Malaysia
*Corresponding author, e-mail: r_rashid47@yahoo.com[1], mfareq@unimap.edu.my[2], hilaladnan@unimap.edu.com[3], weefwenhoon@gmail.com[4]

Abstract

Recently, extensive requirements have developed for ultra-wideband (UWB) technology that provides high activity and small size for use in small communication systems, remote sensing, and radar applications. Thus, we concentrated with high-resolution radar UWB antenna to cover Federal Communication Commission's (FCC) standard UWB range (3.1-10.6 GHz). The proposed ideal-size and low-cost finger-shaped patch antenna of 24 mm x 19 mm printed on 40 mm x 35 mm rectangular Taconic TLY-5 material was designed and established through experiments and simulations. Results show that the two cut notches of 1.5 mm x 2 mm at the bottom corners of the patch can increase the bandwidth. To increase the radiation area and achieve more resonance frequencies, two cut slots at the top edge of the patch were designed in depth of 10 mm. Four parameters were considered in the analysis of the proposed antenna design, namely the feeder width, number of slots, number of notches, and feed gap space. The simulated and measured results of the main antenna parameters make the design suitable in applications of UWB wireless systems.

Keywords: *two notches finger-shaped patch antenna, reflection coefficients, omni-directional patterns, antenna parameters*

1. Introduction

There are many applications for UWB technology at the present time, such as mobile radio and wireless communication with pulses that are less than a nanosecond. UWB techn0logoy is used extensively because it provides several advantages, including 1) low complexity and low cost, 2) high quality service, 3) high transmission rates, and 4) operational flexibility [1]. To meet the requirements of applications in wireless communication systems, small microstrip antennas can be designed that have ultra-wide bandwidths of frequency that allows them to achieve high-capacity bit rates of several hundred Mbps or even Gbps for distances up to 10 meters. The UWB frequencies are allocated by the Federal Communications Commission (FCC) in the United States, and the frequency spectrum ranges from 3.1 to 10.6 GHz with a low-power spectral density of -41.3 dBm/MHz [2]. Thus, we proposed a sensitive microstrip-patch antenna with a reflection coefficient of less than -10 dB that has high gain, good directivity, small size, and transmission-line feeding but which is also lightweight. Many shapes have been designed to achieve the desired UWB characteristics, such as the diamond antenna [3] for the operational band 3.38 to 14 GHz; the T-slotted, ground-plane antenna [4] with a frequency range of 3.1 to 11.5GHz; the 'smart antenna' for spatial rake receivers [5]; UWB slotted microstrip patch antenna using FR4 material of 4.4 dielectric constant and dimensions are 30mm x 55mm [6]; the dual-band, notched antenna with curved was proposed by [7] to operate from 2.5 to 12 GHz; the two-port, circular-patch antenna for divers applications [8]; the bow-tie, planar, wideband dipole with a frequency range between 4 and 9 GHz [9]; a four-element, microstrip, antenna array that was presented in [10] to attract the radiated data in the FCC frequency range; a planar monopole antenna with an octagonal-shaped patch that was produced by [11] and multi-band and wideband antenna was designed by [12] to operate in the allocated bandwidth for UWB wireless communications; fork-shaped radiating patch was proposed by [13] to cover Bluetooth and UWB frequency bands and the fabricated substrate

Received March 7, 2014; Revised April 28, 2014; Accepted May 14, 2014

was made of FR4 material; a four-filter antenna with three split resonators that was suggested to offer dual band WiMAX and WLAN applications [14, 15, 16], while a CPU-fed, planar, inverted-cone antenna was fabricated to cover the bandwidth from 1.3 to 11 GHz with maximum gain [17]. In order to reduce the cost of antennas and also for reducing the cost, antenna was designed in [18] with substrate made of textile material that used to produce jeans, in addition the patch and the ground plane were made of copper to be suitable for UWB bandwidth. A tuning fork type was proposed and simulated by [19] for operating frequency range of 3.7 GHz to 13.8 GHz with printed patch antenna on a FR4 substrate.

In this paper, we concentrated on the design of ultra wideband rectangular patch with two notches on each bottom side of the patch to achieve the bandwidth around 3 GHz to 12 GHz. The antenna had three slots to extend the radiating element reasonably over the operating band 3 - 12 GHz, which is sufficient for UWB operation. The proposed antenna is smaller in size compared with the previous designs to be suitable for small UWB communication systems. In Section 2, detailed design and the dimensions are presented and followed by Section 3 of fabricated antenna design. After that simulated and measured results with their discussions and conclusions are presented in Sections 4 and 5, respectively.

2. Configuration of the Proposed Antenna

The small size and easy to fabricate antennas are two features strongly desired for modern UWB communication systems. Another consideration has to be taken into account is to provide good matching between feed section and radiator part. The geometry of the proposed antenna consists of the following parts, which are suitable for integration with a printed circuit board (PCB).

2.1. The substrate

The length of rectangular microstrip antenna is one-half wavelength if the substrate is air gap and the length decreases when using substrate material of valuable dielectric constant [23]. Taconic TLY-5 material was used in the fabrication of the antenna which was manufactured with very lightweight woven fiberglass and had the following characteristics: dimensional stability; a low dielectric constant range (ε_r = 2.2), a low dissipation factor (approximately 0.0009 at frequency of 10 GHz); made of high-speed digital material; and a wide range of bandwidths. The width, length, and height are denoted by W, L, and h respectively, and the proposed rectangular dimensions were: W = 40 mm, and L = 35 mm, and h = 1.575 mm. The small size of this antenna provides the flexibility required for use in small, wireless communication systems, such as mobile systems, laptop devices, indoor receivers and transmitters, and narrow band radio systems. The effective dielectric constant (ε_{reff}) of the patch was determined to be 2.1 from the following equation [20]:

$$\varepsilon_{reff} = \frac{\varepsilon_r + 1}{2} + \frac{\varepsilon_r - 1}{2\sqrt{1 + (\frac{12h}{W})}} \quad (1)$$

2.2. Ground plane

The rectangular ground plane was made of copper that had a thickness of 0.035 mm, and it was printed on the back of the substrate. The ground plane has a length (L_{gp}) of 11.6 mm and a width (W_{gp}) of 40 mm, which were optimized to obtain the best return loss (S_{11}) (less than -10 dB) and impedance bandwidth. The various dimensions were chosen to increase the effective length bellow the 4 GHz frequency band.

2.3. Feed gap

The bandwidth of the antenna was independent of the feed gap of the ground plane since the ground plane, served as an impedance-matching circuit .The size of the feed gap allowed us to obtain a wider impedance bandwidth and omni-directional radiation patterns .The optimal value of the thickness of the feed gap (L_{gap}) was determined to be 0.4 mm in order to

produce nearly-pure resistive input impedance to cover the UWB range in wireless communication systems.

2.4. Microstrip feed

Four popular configurations are used to feed microstrip antenna, i.e., microstrip line, coaxial probe, aperture coupling, and proximity coupling. The configuration we used in the proposed antenna was the microstrip line feed made of copper with t = 0.035 mm (thickness), L_f = 12 mm (length), and W_f = 4.7 mm (width).

2.5. Microstrip patch element

Many shapes of the microstrip patch have been designed as radiators for UWB radiation. There are two degrees of freedom (length and width) for controlling a rectangular microstrip antenna, so that the order of changing the mode can be done by varying the relative dimensions of the width and length of the patch based on resonant frequency. The patch dimensions of W_p x L_p can be determined according to the following procedure when the resonant frequency (f_r) is 5 GHz [21].

$$W_p = \frac{c}{2 f_r \sqrt{\frac{2}{\varepsilon_r + 1}}} \tag{2}$$

where, c is the speed of the light in free space (3×10^8 m/s), and the width (W_p) of the patch was determined to be 24 mm. The extended length of the patch (ΔL) can be calculated as:

$$\Delta L = 0.412h \frac{(\varepsilon_{reff} + 0.3)(\frac{W_p}{h} + 0.264)}{(\varepsilon_{reff} - 0.258)(\frac{w_p}{h} + 0.8)} \tag{3}$$

The actual length of the patch (L_p) can be calculated by applying equations (4) and (5) to get 19 mm:

$$\lambda_{reff} = \frac{\lambda_r}{\sqrt{\varepsilon_{reff}}} \tag{4}$$

$$L_p = \frac{\lambda_{reff}}{2} - 2\Delta L \tag{5}$$

where λ_r is the resonant wavelength (λ_r = c/f_r) .

Fig. 1 illustrates that each radiating edge of the patch is represented by the admittance (Y) of real part denoted by conductance (G) and the imaginary part denoted by susceptance (B), so that Y = G + jB. To enhance the conventional rectangular UWB antenna, we divided the upper patch edge into three sub-edges (fingers) by making two slots of equal dimensions through the upper patch edge. These three fingers were proposed to increase the radiation area and to get three resonant frequencies that used to expand the bandwidth. For resonant input resistance analysis, the admittances of the fingers are Y_{21}, Y_{22}, and Y_{23}, where $Y_{21} = G_{21} + jB_{21}$, $Y_{22} = G_{22} + jB_{22}$, and $Y_{23} = G_{23} + jB_{23}$. Y_2 is the parallel equivalent admittance of Y_{21}, Y_{22}, and $Y_{23,}$ and it is equal to $G_2 + jB_2$. Since the fingers are identical, $G_2 = G_{21} = G_{22} = G_{23,}$ and $B_2 = B_{21} = B_{22} = B_{23}$, therefore $G_1 = G_2$ and $B_2 = -B_1$. As the total resonant input admittance is real, the total input resistance also is real, and it is given by [22]:

$$Y_{in} = Y_1 + Y_2 = Y_1 + (Y_{21} + Y_{22} + Y_{23}) = G_1 + 3G_2 = 4G_1 \tag{6}$$

$$R_{in} = \frac{1}{Y_{in}} = \frac{1}{4G_1} \tag{7}$$

When the mutual effects are taken into account to calculate the exact value of the input impedance, mutual conductance exists between the edges of the patch, so the input resistance can be expressed as:

$$R_{in}(L_s = 0) = (\frac{1}{4(G_1 \mp G_{12})}) \tag{8}$$

where G_1 is the conductance of the bottom edge of the patch and G_{12} is the mutual conductance between upper and lower edges of the patch. The signs (+) and (-) are used for modes by odd and even resonant voltage distribution, respectively.

$$R_{in}(L_s = value) = R_{in}(L_s = 0)\cos^2(\frac{\pi}{L_p}L_s) \tag{9}$$

where R_{in} (L_s = value) is the input impedance at L_s inset feed point and can be taken as 50 Ω. $R_{in}(L_s = 0)$ is the input impedance at the top edge of the patch, and, when $W_p < \lambda$:

$$G_1 = \frac{1}{90}(\frac{W_p}{\lambda}) \tag{10}$$

The mutual conductance (G_{12}) can be determined by equation (11), where J_0 is the Bessel function of the current density at zero order. By equations (9-11), the depth of each slot (L_s) was calculated to be 10 mm through the antenna patch [20].

$$G_{12} \quad \frac{1}{\pi/2}\int_0^{\pi}[\frac{\sin(\frac{k_0}{2}W_p\cos(\theta))}{\cos(\theta)}]^2 J_0(k_0 L_p \sin(\theta))\sin^2(\theta)d\theta \tag{11}$$

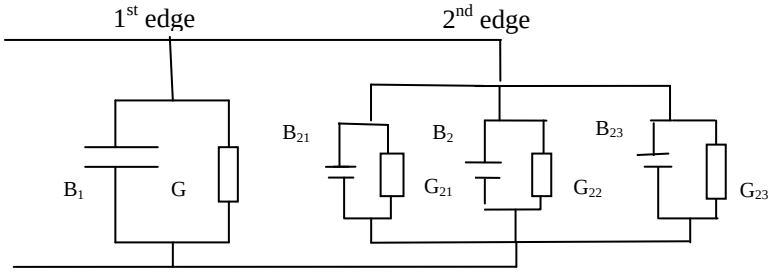

Figure 1. Equivalent circuit of the transmission model

The schematic simulated diagram was derived from the reference rectangular antenna with rectangular printed patch on the front side of the Taconic TLY-5 substrate of thickness 1.575 mm and dielectric constant of 2.2. This geometrical diagram of front and back view is shown in Fig. 2 with all dimensions are defined in Table 1. In this design, there four parameters: feeder width, feed gap space, number of cut slots, and number of cut notches were modified to achieve a wider impedance bandwidth and a better impedance matching.

Table 1. Dimensions of the proposed antenna

Parameters	W	L	W_p	L_p	L_{gp}	θ	L_{gap}	W_f	L_f	W_s	L_s	W_{fing}	R	W_{n1}	L_{n1}	L_{n2}
Value (mm)	40	35	24	19	11.6	45	0.4	4.7	12	3	10	6	3	4	1.5	2

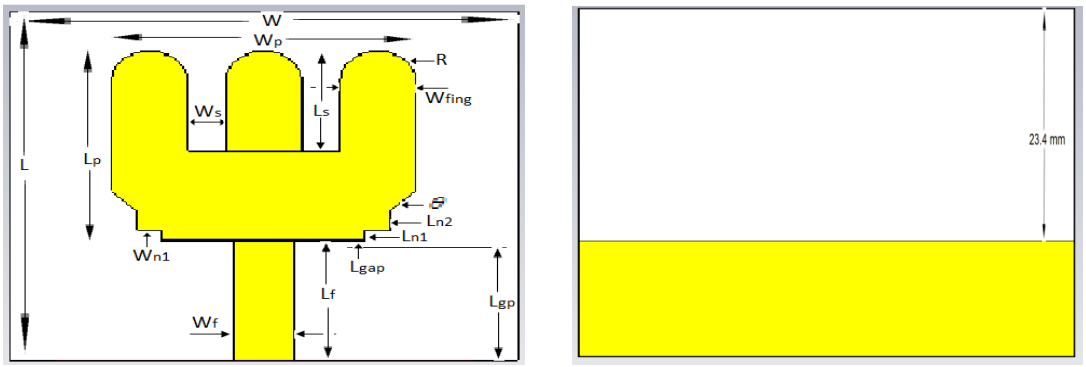

(a) (b)

Figure 2. Dimensions of the proposed antenna (a) front view, (b) back view

3. Geometry of the Fabricated and Printed Antenna

The overall structure of the antenna was successfully fabricated using Taconic TLY-5 material for substrate and copper of 0.035 mm thickness to print radiator and ground plane to be integrated with other system elements. The geometry of the fabricated design is shown in Fig. 3 of prototype mounted on the mentioned material substrate with connector of 50 Ω input impedance.

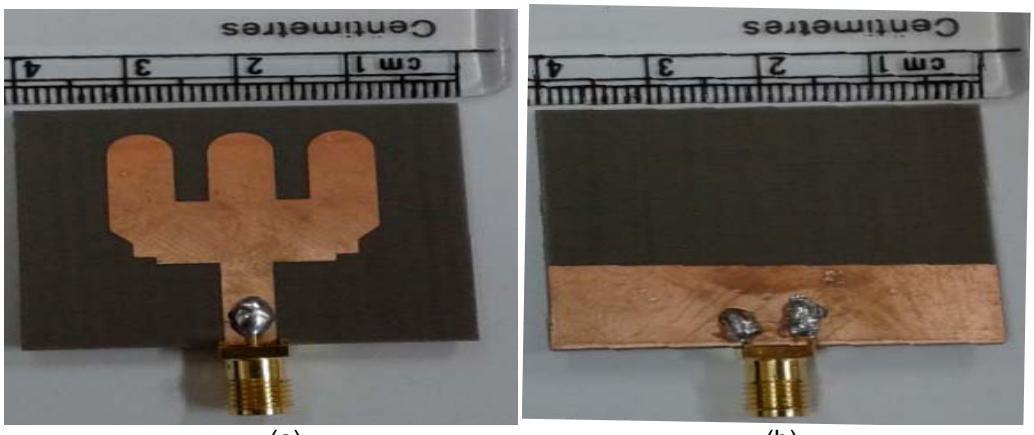

(a) (b)

Figure 3. The fabricated antenna being tested on anechoic chamber and network analyzer: (a) front view; (b) back view

4. Simulated and Practical Results and Discussion for the Proposed Antenna

The performance of an antenna can be measured based on its reduction of the reflection power requirement on the transmission line to the source, which depends on the voltage reflection coefficient at the input terminals of the antenna. The practical and simulation frequency band was 3-12 GHz (ratio bandwidth was 4:1) for the designed antenna to determine its stable radiation characteristics. Fig. 4 illustrates the experimental and simulated return loss

(|S_{11}|dB) against the frequency band of the partially-grounded substrate antenna throughout the UWB frequency. The measured and simulated reflection coefficients (S_{11} < -10 dB) of the antenna are displayed, and they matched the broadband impedance characteristics. The |S_{11}| less than -10 dB bandwidth that from the network analyzer test and the CST software was 3 to 12 GHz within little tolerance variations to give a good estimation of the performance of the antenna. These little losses in the fabrication tolerance and 50 Ω connector caused the variation between the simulated and measured characteristics of S_{11}. From simulated $S_{11,}$ resonance frequencies of 4 GHz, 5 GHz, and 7.6GHz employ at -34 dB, -44dB, and -24dB respectively while in fabricated S_{11}, resonance frequencies of 3.5 GHz, 4.5 GHz, 5 GHz, and 8.1 GHz employ at -35 dB, -33dB, -44dB, and -38dB respectively. Fig. 5 shows the gain characteristics of the proposed antenna versus frequency for the UWB bandwidth. The gain increased as frequency increased and the maximum value occurred at the end of the operating frequency band.

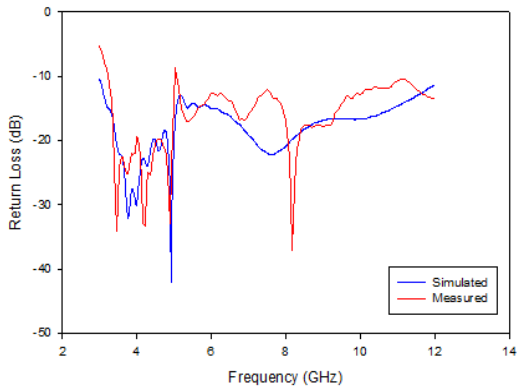

Figure 4. Simulated and measured S_{11} of the proposed antenna

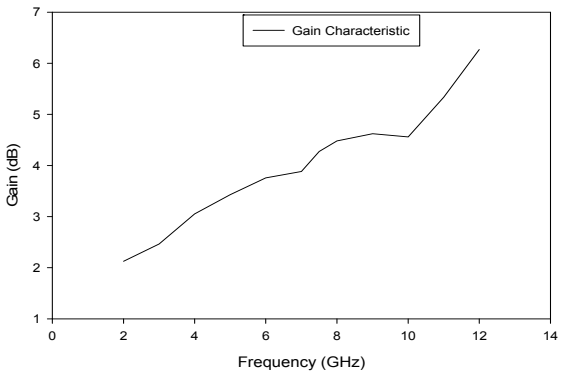

Figure 5. Characteristics of antenna gain with increasing bandwidth for the proposed design

To do antenna design optimization, parametric studies for considered four parameters are shown in Figure 6 when CST Microwave Studio Software was carried out in simulation. In parametric study of each parameter, the CST software was run at various parameters when other parameters were kept invariant. From Fig. 6 (a), the effect of notch cut is illustrated to improve the parameter of using two notches cut at each lower corner of the patch. The return loss curve of two notches is covering the UWB frequency while that of one notch covers up to 8 GHz. Second parameter was proposed is the number of slots at the top edge of the patch. The return loss curves are shown in Fig. 6 (b) with no slot, one slot, and two slots. One can conclude that, a wider impedance bandwidth can be obtained with a patch of two slots at the upper edge in order to cover the UWB bandwidth which is from 3.1 to 10.6 GHz. The other considered parameter is feed gap size (L_{gap}) parameter that was used to optimize the widest bandwidth; the CST software was run at various values of L_{gap}. Fig. 6 (c) shows the calculated return loss curves with three values of L_{gap}. It can be seen that at increasing feed gap size results reductions in bandwidth and return loss. Hence, we conclude that wider impedance bandwidth can be obtained by tuning the feed gap size. After that the software also was run at various feeder width (W_f) values. The results of this variation are presented in Fig. 6 (d) to show the optimal W_f was found to be at 4.7 mm that kept the input impedance equals to 50 Ω, so that no need to decrease or increase W_f and this size is suitable for tolerance with the soldered 50 Ω connector.

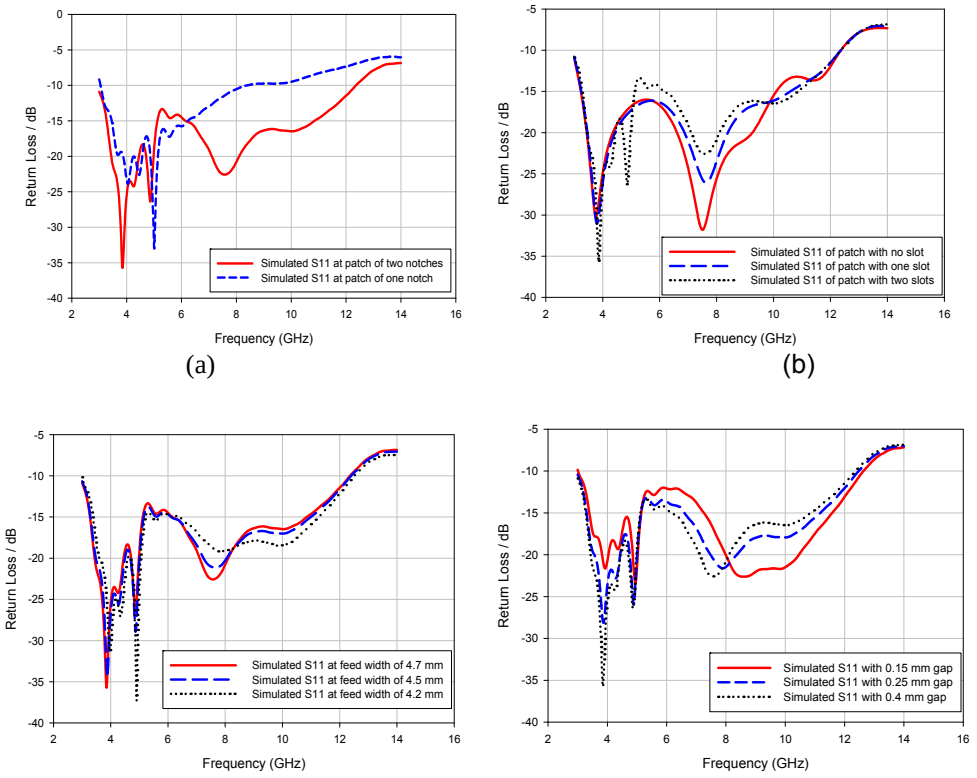

Figure 6. Proposed parametric study; (a) number of notch, (b) number of slot, (c) feeder width, (d) feed gap size

Fig. 7 shows the three-and two-dimensional, omni-directional patterns at frequency of 7.5 GHz, which describe antenna's performance over the entire UWB bandwidth. Simulated current distributions are illustrated in Figure 8 at resonant frequencies of 5 and 3.8 GHz to facilitate the understanding of the antenna's performance. For two set notches and two slots, the figure shows that the surface current on the radiator surface of the antenna was greater at resonant frequency of 5 GHz than that at 3.8 GHz. The peak values of the surface current distribution of the UWB radiator at the notches and the slotted edge was 63.7 A/m at 5 GHz and 23.1 A/m at 3.8 GHz; these values were greater than those presented in [19] at the steppers and convex corners of the radiator. From the simulation results, the values of the proposed antenna design parameters are presented in Table 2 antenna for the chose frequencies over the coverage UWB bandwidth.

Table 2. The values of antenna parameters at specified UWB frequencies

Parameters	4 GHz	6 GHz	8 GHz	10 GHz
S_{11}	-32 dB	-18 dB	-23 dB	-17 dB
Gain	3.062 dB	2.736 dB	4.529 dB	4.516dB
Directivity	2.194	1.933	2.944	2.963
Radiation efficiency	92.26 %	97.13 %	96.38 %	95.47 %
Max power pattern	0.1608 VA/m^2	0.1443 VA/m^2	0.2241VA/m^2	0.2198 VA/m^2

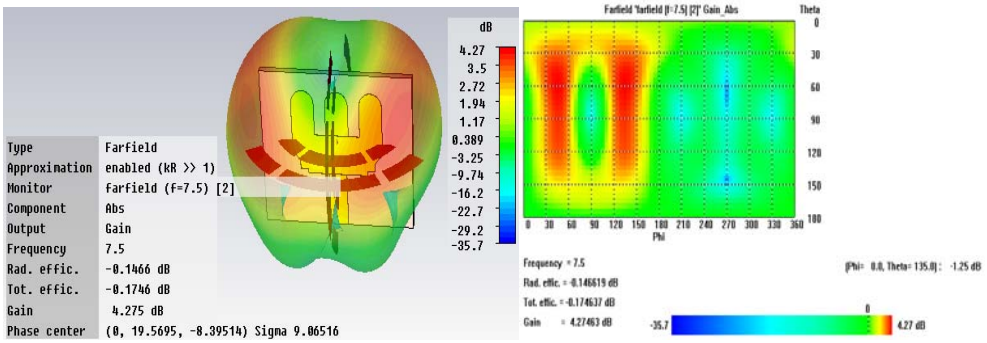

Figure 7. Simulated radiations at 7.5 GHz: (a) three-dimensional radiation pattern; (b) two-dimensional radiation pattern

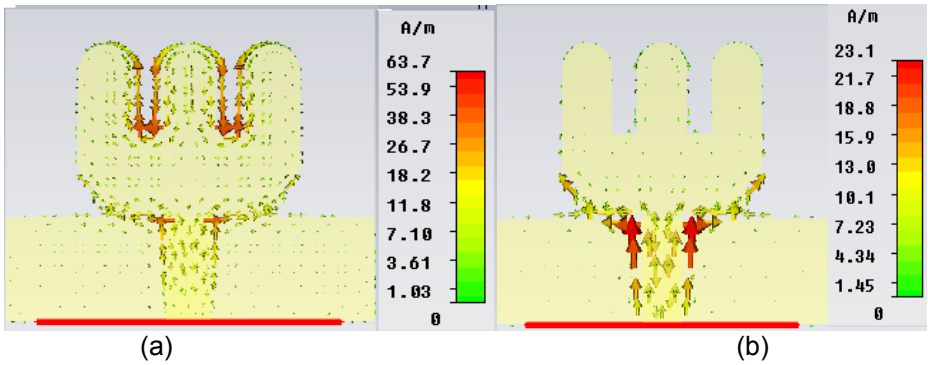

Figure 8. Simulated distribution of current on the surface of the proposed antenna at (a) 5 GHz and (b) 3.8 GHz

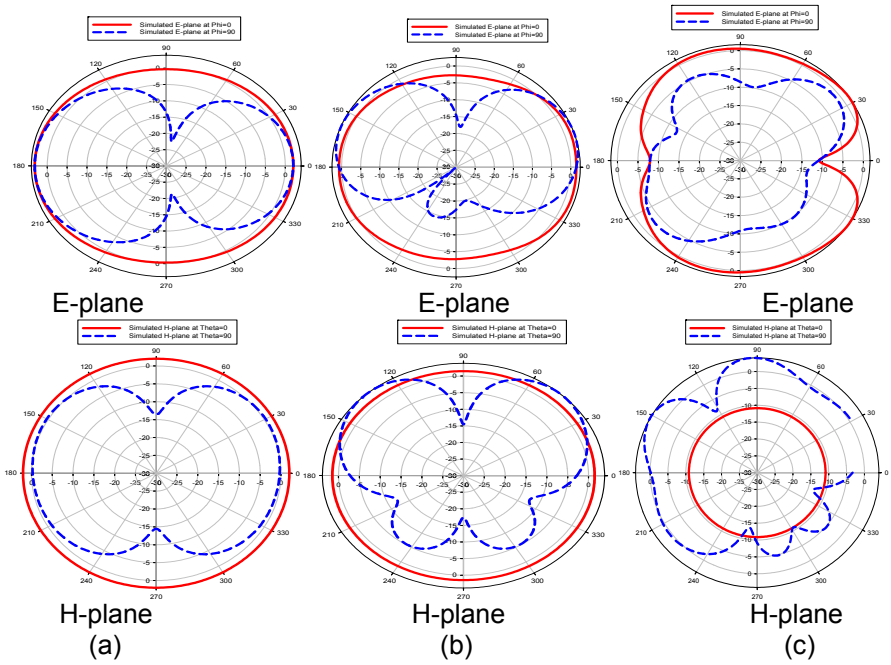

Figure 9. Simulated radiation patterns for E-plane (Phi) and H-plane (Theta) of designed antenna at (a) 4.5 GHz, (b) 7 GHz, and (c) 10 GHz

Fig. 9 shows the simulated radiation patterns of the far-field antenna at the x-y H-plane (Theta = 0^o, 90^o) and at the y-z E-plane (Phi = 0^o, 90^o). These patterns were compared with different values of frequency, i.e., 4.5, 7, and 10 GHz for the H-plane and the E-plane. The radiation patterns essentially were omni-directional in the E and H planes for the simulation of the proposed antenna.

The fabricated antenna was tested using anechoic chamber by fixing the antenna on a stand using 50 Ω connector which is soldered at the lower edge of the feed line. So that by Anechoic chamber and network analyzer, the elevation (E-plane) and azimuth (H-plane) patterns were measured for the proposed antenna in a planes containing feed. These measured radiation patterns are shown in Fig. 10 at three operating frequencies: 4.5 GHz, 7 GHz, and 10 GHz in H-plane (xz-plane) and E-plane (xy-plane) and a little change in patterns due to frequency increase. The measured E-planes and H-planes show mostly omni-directional radiation patterns over the specified frequencies. In measured patterns, there are many ripples at the radiation amplitude due to into the field reflections from antenna holder, chamber scattering, and from inside of the anechoic chamber. To the proposed design with those of [4] and [7], the proposed finger-shaped antenna is smaller in dimension size, higher gain, using lighter and cheaper substrate material, and more stable omni-directional radiation patterns.

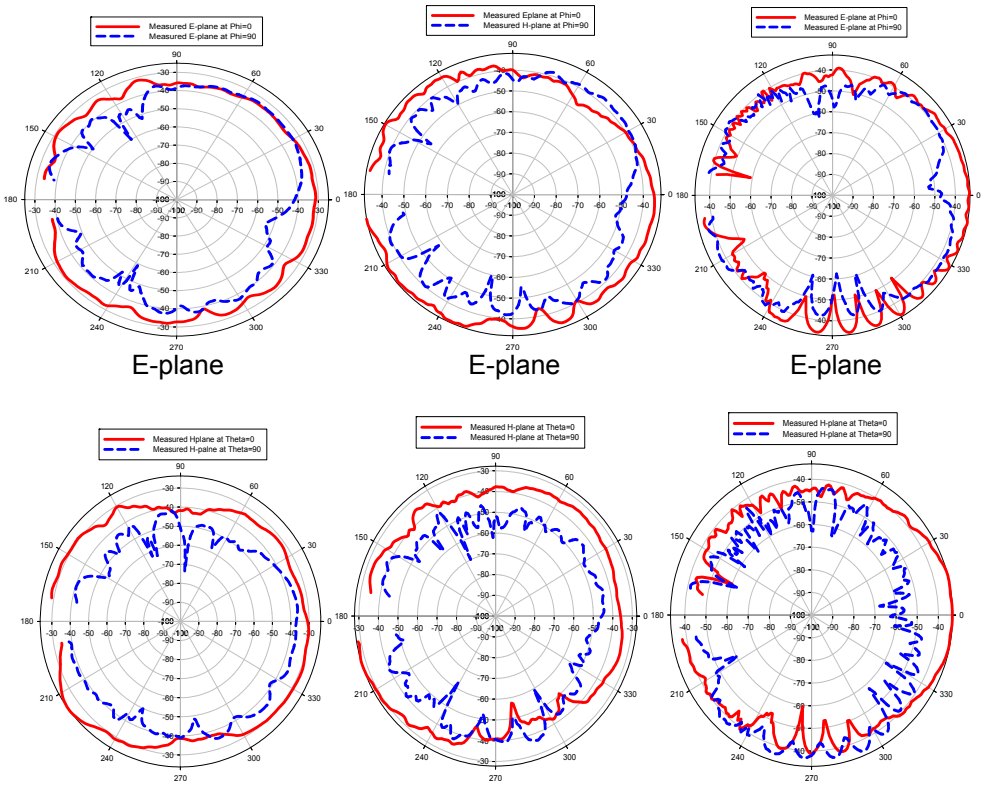

Figure 10. Measured radiation patterns of the fabricated antenna at: (a) 4.5 GHz, (b) 7 GHz, (c) 10 GHz

5. Conclusions

For UWB wireless applications and to reduce costs, a small size of planar finger-shaped patch antenna was designed to cover the wideband frequency range (3 - 12 GHz) to be suitable for indoor and outdoor propagation of wireless UWB communication systems. The cutting slots and notches at the top and bottom edges of the patch radiator contributed to the extension of the radiation area and the evaluation of the current distribution behavior. These cutting slots and notches enhanced the performance of small antenna design over UWB frequency range. The antenna was fabricated and tested, and there was a good agreement between simulated and

measured results for the most important antenna parameters such as return loss (S_{11}<-10 dB) and omni-directional radiation patterns.

References

[1] Mohamed NS .*Chapter 10 in Antenna Handbook of Ultra Wideband Communications: Novel Trends Antennas and Propagation*. University Campus. Shanghai, China. 2011; 09.
[2] AF Molish, K Balakrishnan, D Cassioli, CC Chong, S Emami, J Karedal. *IEEE 802.15.4a Channel Model-Final report. Task group 4a (TG4a), Tech. Report*, 2004.
[3] Zaini KD, Meriah SM. New Diamond Antenna for Ultra Wideband Applications. *IJCSI International Journal of Computer Science Issues.* 2012; 9(4).
[4] Yusnita R, Razali N, Tharek AR. *Chapter 18 of Ultra Wideband Handbook*. University Campus. Shanghai. China. 2010.
[5] Hans GS. Smart Antenna for Spatial Rake UWB Systems. *IEEE conference on ultra wideband systems and technologies.* 2004.
[6] Tajeswita G, PK Singhal. Ultra Wideband Slotted Microstrip Patch Antenna for Downlink and Uplink Satellite Application in C band. *International Journal of Innovation and Applied Studies*. 2013; 3(3): 680-684.
[7] A Karmarkar, S Verma, M Pal, R Ghatak. An Ultra Wideband Monopole Antenna with Multiple Fractal Slots with Dual Band Rejection Characteristics. *Progress In Electromagnetics Research.* 2012; 31: 185-196.
[8] E Antonino-Daviu, M Gallo, M Cabedo-Fabres, M Ferrando-Bataller. Novel Ultra Wideband Antenna for Diversity Applications. *IEEE Conference.* Bari. Italy. 2010.
[9] AD Capobianco, FM Pigozzo, A Locatelli, D Modotto. *Chapter 1 (Directive Ultra-Wideband Antennas) in Microwave and Millimeter Wave Technologies Modern UWB Antennas and Equipment Handbook*. University Campus. Shanghai. China. 2010.
[10] B Kasi, CK Chakrabarty. Ultra-Wideband Antenna Array Design for Target Detection. *Progress in Electromagnetics Research.* 2012; 25: 67-79.
[11] MY Alhefnawy, Aladdin A, Hosny A, A Safwat, MI Youssef. Design and Implementation of a Novel Planar UWB Monopole Antenna for Multipath Environments. *13th International Conference on Aerospace Sciences & Aviation Technology,* Cairo, Egypt. 2009.
[12] H Oraizi, B Rezaei. Combline Loadings of Printed Triangular Monopole Antennas for the Realization of Multi-Band and Wideband Characteristics. *Progress In Electromagnetic Research B.* 2012; 39: 179-195.
[13] Mishra SK, Gupta RK, Vaidya A, Mukherjee J. Printed Fork Shaped Dual Band Monopole Antenna for Bluetooth and UWB Applications With 5.5GHz WLAND Band Notched Characteristics. *Progress In Electromagnetics Research C*. 2011; 22: 195-210.
[14] DO Kim, NI Jo, HA Jang, CY Kim. Design of the Ultra Wideband Antenna with a Quadruple-Band Rejection Characteristics Using a Combination of the Complementary Split Ring Resonators. *Progress In Electromagnetics Research.* 2011; 112: 93-107.
[15] P Tilanthe, PC Sharma, TK Bandopadhyay. A Monopole Microstrip Antenna with Enhanced Dual Band Rejection for UWB Applications. *Progress In Electromagnetics Research.* 2012; 38: 315-331.
[16] Y Zhuo, L Yan, X Zhao, K Huang. A Compact Dual-Band Patch Antenna for WLAN Applications. *Progress In Electromagnetics Research Letters.* 2011; 26: 153-160.
[17] Jia L, Shu L, Yu T, Liwen J, Mengqian L, Zhihua Z. The Simulation and Experiment of a UWB Printed Dipole Antenna. *Progress In Electromagnetics Research Letters.* 2013; 36: 21-30.
[18] Mai AR, Osman M, KA Rahim, M Azfar, NA Samsuri, F Zubir, K Kamardin. Design Implementation and Performance of Ultra-Wideband Textile Antenna. *Progress In Electromagnetics Research B.* 2011; 27: 307-325.
[19] AHM Zahirul A, Rafiqul I, Sheroz K. Design of a Tuning Fork type UWB Patch Antenna. *Int. Journal of Electrical and Electronics Engineering*. 2006: 1-8.
[20] CA Balanis. *Antenna Theory: Analysis and Design*. By John Wiley & Sons. INC. 2013.
[21] KK Parashar. Design and Analysis of I-Slotted Rectangular Microstrip Patch Antenna for Wireless Application. *International Journal of Electrical and Computer Engineering (IJECE).* 2014; 4(1): 31-36.
[22] WF Richards. Microstrip Antennas, Chapter 10 in Antenna Handbook: Theory, Applications and Design. *Van Nostrand Reinhold Co*. New York. 1988.
[23] MM Ahamed, K Bhowmik, M Shahidulla, MS Islam, MA Rahman. Design and Analysis of I-Slotted Rectangular Microstrip Patch Antenna for Wireless Application. *International Journal of Electrical and Computer Engineering (IJECE).* 2012; 2(3): 417-424.